Carbohydrate Polymers 94 (2013) 567–576

Contents lists available at SciVerse ScienceDirect

Carbohydrate Polymers

journal homepage: www.elsevier.com/locate/carbpol

Branching pattern of gluco-oligosaccharides and 1.5 kDa dextran grafted by the α-1,2 branching sucrase GBD-CD2

Yoann Brison[a,b,c], Sandrine Laguerre[a,b,c], François Lefoulon[d], Sandrine Morel[a,b,c], Nelly Monties[a,b,c], Gabrielle Potocki-Véronèse[a,b,c], Pierre Monsan[a,b,c], Magali Remaud-Simeon[a,b,c,*]

[a] Université de Toulouse; INSA, UPS, INP; LISBP, 135 Avenue de Rangueil, F-31077 Toulouse, France
[b] CNRS, UMR5504, F-31400 Toulouse, France
[c] INRA, UMR792 Ingénierie des Systèmes Biologiques et des Procédés, F-3140 Toulouse, France
[d] Technologie Servier, 25/27 rue Eugène Vignat, 45000 Orléans, France

ARTICLE INFO

Article history:
Received 27 November 2012
Received in revised form 20 January 2013
Accepted 21 January 2013
Available online 28 January 2013

Keywords:
Glucansucrase
α-(1 → 2) Branching sucrase
Sucrose
Gluco-oligosaccharides
Dextran
Prebiotics

ABSTRACT

GBD-CD2, an engineered sucrose-acting enzyme of glycoside hydrolase family 70, transfers D-glucopyranosyl (D-Glc*p*) units from sucrose onto dextrans or gluco-oligosaccharides (GOS) through the formation of α-(1 → 2) linkages leading to branched products of interest for health, food and cosmetic applications. Structural characterization of the branched products obtained from sucrose and pure GOS of degree of polymerization (DP) 4 or DP 5 revealed that highly α-(1 → 2) branched and new molecular structures can be synthesized by GBD-CD2. The formation of α-(1 → 2) branching is kinetically controlled and can occur onto vicinal α-(1 → 6)-linked D-Glc*p* residues. To investigate the mode of branching of 1.5 kDa dextran, simulations of various branching scenarios and resistance to glucoamylase degradation were performed. Analysis of the simulation results suggests that the branching process is stochastic and indicates that the enzyme acceptor site can accommodate both linear and poly-branched acceptors. This opens the way to the design of novel enzyme-based processes yielding carbohydrate structures varying in size and resistance to hydrolytic enzymes.

1. Introduction

Glucansucrases (EC 2.4.1.5) produced by lactic acid bacteria of the genera *Leuconostoc*, *Lactobacillus*, *Streptococcus* and *Weissella* are transglucosylases that use sucrose, a cheap agro-resource, to synthesize polymers of D-glucopyranosyl units (D-Glc*p*) named α-glucans. The type and the percentage of α-(1 → 2), α-(1 → 3), α-(1 → 4) or α-(1 → 6) glucosidic linkages vary, depending on the enzyme specificity (Bounaix et al., 2009; van Hijum, Kralj, Ozimek, Dijkhuizen, & van Geel-Schutten, 2006; Malik, Radji, Kralj, & Dijkhuizen, 2009; Monchois, Willemot, & Monsan, 1999). Classified in family 70 of glycoside-hydrolases in the CAZy database, glucansucrases share the same α-retaining mechanism involving the formation of a β-D-Glc*p*-enzyme intermediate from sucrose cleavage (Cantarel et al., 2009; Henrissat & Davies, 1997; Mooser, Hefta, Paxton, Shively, & Lee, 1991; Vujičić-Žagar et al., 2010). These enzymes also catalyse the transfer of D-Glc*p* moieties from the sucrose donor onto a wide variety of acceptor molecules in what is so called "acceptor reactions" (Bertrand et al., 2006; Côté, Dunlap, & Vermillion, 2009; Moon et al., 2007). Gluco-oligosaccharides (GOS) or gluco-conjugates may be produced depending on the acceptor structure (André et al., 2010; Iliev et al., 2008). Glucansucrase activity from *Leuconostoc mesenteroides* NRRL B-1299 is responsible for the production of an original dextran with 61% of α-(1 → 6) linkages, 12% of α-(1 → 3) linkages and 28% of α-(1 → 2) linkages (Fabre et al., 2005; Kobayashi & Matsuda, 1977; Seymour, Knapp, Chen, Bishop, & Jeanes, 1979). From sucrose and maltose used as acceptor, a mixture of GOS is synthesized. Some of them are only composed of α-(1 → 6)-linked D-Glc*p* residues attached to the non-reducing end of maltose. Other series of GOS contain additional α-(1 → 2) osidic linkages (Dols, Simeon, Willemot, Vignon, & Monsan, 1997). The rare α-(1 → 2) glucosidic bond is of particular interest as it is resistant to human and animal digestive enzymes, and confers prebiotic properties to these compounds which are marketed as food, feed and dermo-cosmetic ingredients (Boucher et al., 2003; Djouzi & Andlueux, 1997; Flickinger et al., 2000; Sanz, Côté, Gibson, & Rastall, 2006; Sarbini et al., 2011; Valette et al., 2006).

Abbreviations: CD, catalytic domain; DP, degree of polymerization; GBD, glucan binding domain; GH, glycoside hydrolase; Glc*p*, glucopyranosyl; GOS, gluco-oligosaccharide; HPAEC-PAD, high performance anion exchange chromatography – pulsed amperometric detection; IMOS, isomalto-oligosaccharide.

* Corresponding author at: Laboratoire d'Ingénierie des Systèmes Biologiques et des Procédés, Institut National des Sciences Appliquées, 135 Avenue de Rangueil, 31077 Toulouse Cedex, France. Tel.: +33 561 559 446; fax: +33 561 559 400.
E-mail addresses: remaud@insa-toulouse.fr, magali.remaud@insa-toulouse.fr (M. Remaud-Simeon).

0144-8617/$ – see front matter © 2013 Elsevier Ltd. All rights reserved.
http://dx.doi.org/10.1016/j.carbpol.2013.01.064

To date, only three α-(1 → 2) branched GOS molecules of degree of polymerization (DP) 4, 5 or 6 have been structurally characterized using ^{13}C and ^{1}H NMR analyses (Dols et al., 1997; Remaud-Simeon, Lopez-Munguia, Pelenc, Paul, & Monsan, 1994). The tetrasaccharide and pentasaccharide were shown to both possess a terminal α-(1 → 2) linked D-Glc*p* unit at their non-reducing extremity whereas the hexasaccharide shows an α-(1 → 2)-linked D-Glc*p* unit attached to the ante penultimate D-Glc*p* residue from the non-reducing end (Dols et al., 1997). No further structural characterizations of the α-(1 → 2) branched GOS have been reported. Indeed, the preparation of pure products was hampered by the presence of both linear and branched GOS in the reaction mixtures. This was because *L. mesenteroides* NRRL B-1299 native glucansucrase (DSR-E dextransucrase; 313 kDa) is a polyspecific enzyme that synthesizes α-(1 → 6), α-(1 → 3) and α-(1 → 2) linkages.

DSR-E encoding gene (GenBank accession number AJ430204) was identified and expressed in *Escherichia coli* (Bozonnet et al., 2002). DSR-E sequence analysis revealed the presence of two catalytic domains (CD1 and CD2) separated by a glucan binding domain (GBD) (Fabre et al., 2005). Several truncated forms of DSR-E were constructed and one of them, referred as GBD-CD2, was proved to be involved in the formation of the α-(1 → 2) linkage (Fabre et al., 2005). This opened the way to more detailed biochemical and structural characterization of the α-(1 → 2) branching activity. The three dimensional structure of a shorter truncated active enzyme form was recently solved at 1.9 Å resolution (Brison et al., 2012).

From sucrose only, GBD-CD2 is unable to synthesize glucan and only acts as a sucrose hydrolase. In the presence of sucrose and dextrans as acceptors, glucosylation of α-(1 → 6)-linked D-Glc*p* units through the formation of α-(1 → 2) linkages is observed (Fabre et al., 2005). This reaction proceeds via a ping pong bi bi mechanism and the α-(1 → 2) linkage content in dextrans can be controlled by modulating the [sucrose]/[dextran] molar ratio (Brison et al., 2010). The resulting products are very promising dietary fibres as they show a much higher resistance to digestive enzymes than the linear α-(1 → 6)-linked GOS. In addition, they are selectively fermented by beneficial human gut bacteria (Sarbini et al., 2011) and could be used to control or prevent metabolic diseases (Serino et al., 2012). Despite their interest for health, food and feed industries, the panel of branched oligosaccharide and polysaccharide structures that can be synthesized by GBD-CD2 was never characterized in details. Such structural investigations are necessary to deepen the understanding of GBD-CD2 structure-function relations. It is also a pre-requisite to optimize both enzyme design and production process for synthesizing dietary fibres with defined structures and properties. Herein, we describe the structural characterization of the acceptor reaction products synthesized by the α-(1 → 2) branching sucrase GBD-CD2 in the presence of pure linear GOS of defined degree of polymerization. As the synthesis process of α-(1 → 2)-branched products may also be based on glucosylation of short dextran chains (Brison et al., 2010), we investigated the branching process of 1.5 kDa chains by modelling several branching scenarios leading to variable resistance to amyloglucosidase digestion. The results of our simulations were compared to experimental data and are discussed with regards to enzyme specificity.

2. Materials and methods

2.1. Production and purification of the GBD-CD2 enzyme and DSR-S dextransucrase

Methods for recombinant production in *E. coli* and purification of the branching sucrase GBD-CD2 were previously described (Brison et al., 2010). DSR-S dextransucrase (EC 2.4.1.5) from *L. mesenteroides* NRRL B-512F was produced and purified as previously described (Lopez & Monsan, 1980; Paul, Oriol, Auriol, & Monsan, 1986).

2.2. Enzymatic activity assay of the GBD-CD2 branching sucrase

One enzymatic unit is defined as the amount of enzyme which catalyses the hydrolysis of 1 μmol of sucrose per minute at 30 °C in 20 mM sodium acetate buffer, pH 5.75, with sucrose at the initial concentration of 292 mM. In the presence of sucrose alone, GBD-CD2 releases fructose and glucose that are monitored using the dinitrosalicylic acid method (Sumner & Howells, 1935).

2.3. Production and purification of tetrasaccharide **1** and pentasaccharide **4**

The GOS were produced at 30 °C using native DSR-S at 2000 U kg^{-1} of reaction medium, from sucrose at 200 g kg^{-1} of reaction medium and maltose at 66 g kg^{-1} of reaction medium in 20 mM sodium acetate buffer, pH 5.4. When all sucrose was depleted, the reaction was stopped by thermal inactivation of the enzyme at 95 °C. One volume of the final reaction medium was mixed overnight with one volume of ethanol 95% to precipitate co-produced high molecular weight dextran at 4 °C. The supernatant containing GOS was recovered by centrifugation at 15,241 × *g* during 10 min at 4 °C. Ethanol was removed by evaporation. The resulting GOS solution, containing the GOS **1** and **4**, was cleared out of glucose, fructose, disaccharides and panose by preparative ion exchange chromatography using an Amberlite® CR1320K resin (Rohm and Haas, Philadelphia, USA) packed in an 11 cm × 100 cm double-walled column and distilled water at a flow rate of 80 mL min^{-1} as mobile phase. The column temperature was set at 60 °C. The injection volume is 250 mL at a total sugar concentration of 400 g L^{-1}. The eluted saccharides were detected by refractometry. The fractions containing GOS with a DP superior to three were pooled and freeze-dried. Preparative chromatography using Synergi Fusion RP (10 μm; 80 Å; Phenomenex) as stationary phase packed in a 40 mm × 500 mm column was performed to separate and isolate each GOS. The chromatography was carried out at room temperature using distilled water at a flow rate of 50 mL min^{-1} with a refractometer as detector. The injection volume was 5 mL at a sugar concentration of 300 g L^{-1}. The GOS **1** or **4** were pure at 99%.

2.4. Production and purification of α-(1 → 2) branched GOS **1** or **4**

Pure GOS **1** or **4** were individually branched with GBD-CD2 in the following conditions: sucrose 100 g kg^{-1} of reaction medium, pure tetrasaccharide **1** at 25 g kg^{-1} of reaction medium or pentasaccharide **4** at 30 g kg^{-1} of reaction medium, GBD-CD2 at 2000 U kg^{-1} of reaction medium, 20 mM sodium acetate buffer, pH 5.4, temperature 30 °C. Purifications of α-(1 → 2)-branched GOS **1** or **4** were carried out in the same conditions as those used for unbranched GOS.

For analytical purposes and determination of initial reaction velocities, glucosylation reactions of GOS **1** or **4** were also carried out in the following conditions: 292 mM sucrose, acceptor GOS **1** or **4** at a concentration of 40 mM, 1 U mL^{-1} of GBD-CD2, 30 °C, in 20 mM sodium acetate buffer at pH 5.75 during 24 h. For initial velocity determinations, the enzyme concentration was lowered to 0.1 U mL^{-1}.

2.5. Enzymatic synthesis of dextrans with controlled amounts of α-(1 → 2) linkages

Dextrans with 5–25% of α-(1 → 2) branches were synthesized, as previously described, from 1.5 kDa dextran (M_p 1586 g mol^{-1}, M_w 2111 g mol^{-1}, M_n 755 g mol^{-1}, M_z 4533 g mol^{-1}, M_w/M_n = 2.80, Fluka, Biochemika) (Brison et al., 2010). Aliquots were withdrawn from the reaction mixture at the initial and final reaction times for subsequent enzymatic degradations. Endodextranase (6-α-D-glucan 6-glucanohydrolase; EC 3.2.1.11; from *Chaetomium gracile*, Sankyo Co) was used at 3 U mL^{-1} of reaction media and the mixture was incubated at 37 °C (Hattori, Ishibashi, & Minato, 1981). Degradation with amyloglucosidase from *Aspergillus niger* (glucan 1,4-alpha-glucosidase; EC 3.2.1.3; Sigma–Aldrich) was performed with enzyme concentrations varying from 25 to 9 U mL^{-1} depending on the amount of dextran to be hydrolysed, at 60 °C (Pazur & Ando, 1960). Aliquots of the reaction media were heat inactivated at 95 °C for 15 min before analysis by HPAEC-PAD. The degradation of the α-(1 → 2) branched products obtained from tetrasaccharide **4** was performed in the same conditions.

2.6. Analytic chromatography

2.6.1. GOS analyses by HPLC and LC–MS

GOS were separated at 30 °C by HPLC on a Dionex System equipped with refractometer and a Synergi Fusion RP column (4 μm; 80 Å; 250 mm × 4.6 mm Phenomenex) using ultrapure water as eluent at 0.5 mL min^{-1}. This system was coupled to a MSQ® Plus Mass Spectrometer (Dionex – Thermoscientific equipment) for LC–MS analysis. The molecules were ionized by electrospray ionization technique with a source at 450 °C. Separation was achieved with a quadripole and we used the positive mode for detection.

2.6.2. Glucose and fructose assays for initial velocity determinations

The initial velocities of sucrose consumption and glucose (or fructose) productions were determined from saccharide quantitation with the HPLC system described above, using an Aminex HPX-87C Carbohydrate column (300 mm × 7.7 mm; Bio-rad, Hercules, CA, USA). The fructose production rates reflect the total enzymatic activity whereas fructose minus glucose production rate is representative of the transferase activity.

2.6.3. HPAEC-PAD analyses

HPAEC-PAD analyses were carried out as described by Fabre et al. using a CarboPac™ PA100 (4 mm × 250 mm) analytical column with a CarboPac™ PA-100 Guard (4 mm × 50 mm) (Fabre et al., 2005). For α-(1 → 2) branched 1.5 kDa dextrans, the sodium acetate gradient was applied as follows: from 6 mM to 300 mM in 30 min and from 300 mM to 6 mM in 5 min. The dextrans were prepared in ultrapure water at a final concentration of 40 mg L^{-1}. Glucose, fructose, sucrose, leucrose, isomaltose and isomaltotriose were used as standards for quantitation.

2.6.4. Determination of IMOS content in dextran 1.5 kDa

The concentrations of monosaccharides and isomalto-oligosaccharides (IMOS) in 1.5 kDa dextran solutions were determined by HPLC using a Synergi Fusion RP column (4 μm; 80 Å; 250 mm × 4.6 mm Phenomenex) equipped with a refractometer. Dextran 1.5 kDa, isomaltose, isomaltotriose and D-glucose were dried out during 3 days at 45 °C before dissolution in ultrapure water. Solutions of 1.5 kDa dextran were injected at 49.23 and 97.36 g L^{-1}. Using ultrapure water as eluent, IMOS from DP1 to DP10 were separated in 85 min. D-glucose, isomaltose and isomaltotriose (Aldrich) were used as standards. Using water–methanol eluent (96/4, v/v), the IMOS from DP4 to DP31 were separated in 90 min. We observed a difference of 4.4% (w/w) between the IMOS quantified by HPLC and the IMOS weighted for the preparation of the 1.5 kDa dextran solution. Using this IMOS quantitation in 1.5 kDa dextran (i) M_n, M_w and M_z calculated values are 901, 1432 and 1995 g mol^{-1}, respectively and (ii) the proportions of each IMOS in 1.5 kDa dextran were calculated.

2.7. 1D and 2D NMR analysis

Samples were exchanged twice with 99.9 atom% D_2O, lyophilized and dissolved in 600 μL D_2O. All 1D NMR spectra were recorded at 298 K on an Avance II (Bruker) 500 MHz spectrometer (500 MHz for ^{1}H NMR and 125 MHz for ^{13}C NMR) using a 5 mm z-gradient TBI probe. Data were acquired and processed using topspin 2.1 software. 1D ^{1}H NMR spectra were acquired by using a 30° pulse, 8000 Hz sweep width and 5 s total relaxation delay. A total of 16 scans were recorded. 1D ^{13}C NMR spectra were recorded using an inverse gated sequence taken from the Bruker pulse sequence library, and using a 90° pulse, 25,000 Hz sweep width, 2.5 s relaxation delay and 0.63 s acquisition time.

Heteronuclear multiple bond correlation spectroscopy (HMBC) experiments were recorded on a Bruker Avance 400 spectrometer (proton frequency of 400.13 MHz and ^{13}C frequency of 100.62 MHz) using the Bruker standard pulses programme. The delay time for evolution of long-range ^{13}C–^{1}H couplings was set to 120 ms. Typically, parameters used were 1200 Hz spectral width for ^{1}H and 22,130 Hz for ^{13}C, 16 scans and 196 experiments were accumulated, respectively. Samples were analyzed at 300 K in 5 mm o.d. tubes. Chemical shifts are given using an external reference (d6-trimethylsillylpropionic acid, sodium salt).

2.8. High resolution mass spectrometry

2.8.1. Sample preparation

The samples were dissolved (0.01 mg mL^{-1}) in a methanol/water 50:50 (v/v) mixture and the solutions obtained were injected (5 μL min^{-1}) with a syringe pump (Harvard Apparatus) into the electrospray source.

2.8.2. Mass spectrometry

Infusion electrospray mass spectra in the positive mode were obtained on a Waters-Micromass Q-TOF2 and a Waters-Micromass LC–TOF equipped with a pneumatically assisted electrospray (Z-spray) ion source. The source and desolvatation temperatures were kept at 80 °C and 120 °C respectively. Nitrogen was used as drying and nebulizing gas at flow rates of 500 L h^{-1} and 20 L h^{-1} respectively. The capillary voltage was 3.0 kV and cone voltage 35 V. For collision-induced dissociation experiments (CID), argon was used as collision gas at an indicated analyzer pressure of 5×10^{-5} Torr and the collision energy was set to 85 V.

2.8.3. Modelling of the branching scenarios

To investigate how GBD-CD2 tranfers the D-Glc*p* units to 1.5 kDa dextran, we have developed a PERL programme allowing first the simulation of α-(1 → 2) different branching scenarios according to three criteria: (i) the chain selection by the enzyme, (ii) the direction of branching progress and (iii) the branching pattern (Table 1). Then, programme implementation also enabled the degradation of the branched dextran by glucoamylase to be simulated and the results to be compared to experimental data.

2.8.4. Simulations consisted in a three step strategy

2.8.4.1. Construction of the dextran model. The proportion of each IMOS in the 1.5 kDa dextran population, which was used as substrate, was first determined considering the IMOS of DP ranging from 1 to 61. The IMOS from DP 32 to 61, of which the presence

Table 1
Modelling of branching scenarios.

Scenario	Chain selection[a]				Branching direction[b]			Branching pattern[c]		
	CS1	CS2	CS3	CS4	BD1	BD2	BD3	BP1	BP2	BP3
A	√				√			√		
B	√				√			√[d]		
C	√				√				√	
D	√				√					√
E	√					√		√		
F	√						√	√		
G		√			√			√		
H		√			√			√[d]		
I		√			√				√	
J		√			√					√
K		√				√		√		
L		√					√	√		
M			√		√			√		
N			√		√			√[d]		
O			√		√				√	
P			√		√					√
Q			√			√		√		
R			√				√	√		
S				√		√		√		
T				√			√	√		

For each line, √ stands for a set of conditions gathered for a specific scenario.

[a] Chain selection: • CS1: random selection of IMOS chains; • CS2: random selection of IMOS chains and no more than three branching events occurring on a single chain, i.e. if it already contains three branches, its selection is rejected and another chain is randomly selected; • CS3: random selection of IMOS chains with a probability of branching event increasing with the degree of polymerization (DP2 has two times more chance to be selected than DP1, DP3 3 times . . .); • CS4: random selection of IMOS chains and progressive branching until "completion" of the chain (the chain is not released before it is fully branched, only after this can another chain be selected).

[b] Branching direction: • BD1: no specific direction (random); • BD2: from the non-reducing extremity of IMOS chains; • BD3: from the reducing extremity of IMOS chains.

[c] Branching pattern: • BP1: no particular pattern; • BP2: one unbranched residue between two branched ones.

[d] Scenarios for which there is no specific branching pattern, as in scenario A. However, the last two positions of each chain cannot be branched.

In all the simulated scenarios, DP1 (D-glucose) is not branched as based on experimental data (data not shown).

is detected by HPAEC-PAD, were neglected as they represent less than 2.3% (w/w) of the IMOS population. Based on these assumptions, we generated a data matrix (supplementary data, Fig. S1a) of m lines ($1 \le i \le m$) and n columns ($1 \le j \le n$) where m represents the total number of IMOS molecules in the dextran model and n the maximum DP. Thus, n is equal to 31 which is the maximum DP of the quantified IMOS. Each line in the matrix represents one single IMOS molecule. In this matrix, $a_{i,j}$ is the variable representing one of the D-Glc*p* units of the IMOS molecule. The $a_{i,j}$ value is 1 when there is a D-Glc*p* unit at the corresponding position. Otherwise, it takes the 0 value. For instance, for isomaltopentaose $a_{i,j}$ is equal to 1 in the five first columns of the matrix since there are five D-Glc*p* units in isomaltopentaose. In the other 26 remaining columns, $a_{i,j}$ is equal to 0.

The proportion of each DP in the biological substrate was determined from HPLC quantitation data. To simulate the substrate, we have multiplied all observed molar concentrations of IMOS from DP 1–31 by 1,000,000, so that the simulated substrate would contain 9 molecules of the less represented IMOS (DP 31) and that the total number of IMOS molecules with DP from 1 to 31 would be 99,104. Glucose molecules (11,193 in total) were then excluded of the simulations since they cannot be used as acceptor by GBD-CD2.

2.8.4.2. Simulation of the α-(1 → 2) branching mode. The previously described substrate matrix was used for modelling the α-(1 → 2) dextran branching reaction catalysed by GBD-CD2 (supplementary data, Fig. S1b and c). According to the branching scenarios tested, programmes change $a_{i,j}$ values from 1 to 2 when an α-(1 → 6)-linked D-Glc*p* unit of IMOS was considered as branched.

2.8.4.3. Simulation of the enzymatic degradation. As amyloglucosidase does not hydrolyse α-(1 → 2) linkages and acts from the non-reducing substrate extremity, virtual D-Glc*p* units were released and counted until the programme encounters $a_{i,j}$ having a value of 2. Then, for each simulation, the percentage of released glucose was calculated as being the ratio between the number of released glucose molecules and the number of anhydroglucosyl units in undigested α-(1 → 2) branched dextrans. The same formula was used for experimental data.

One hundred simulations were performed for each experimental branching ratio tested with each branching scenario. The results were summarized in terms of means and standard deviations for the percentage of released glucose. The stability observed over the simulations showed that the number of simulations was sufficient to draw conclusions.

3. Results and discussion

3.1. Glucosylation pattern of tetrasaccharide *1* and pentasaccharide *4*

The first aim was to characterize the GBD-CD2 mode of branching of linear α-(1 → 6) linked GOS presenting a maltosyl residue at their reducing end. First, we characterized by LC–MS, ^{1}H NMR, HMQC and HMBC, the structure of the α-(1 → 2) branched GOS successively obtained from acceptor reactions in the presence of sucrose and pure tetrasaccharide **1** (α-D-Glc*p*-(1 → 6)-α-D-Glc*p*-(1 → 6)-α-D-Glc*p*-(1 → 4)-D-Glc*p*) or pentasaccharide **4** (α-D-Glc*p*-(1 → 6)-α-D-Glc*p*-(1 → 6)-α-D-Glc*p*-(1 → 6)-α-D-Glc*p*-(1 → 4)-D-Glc*p*).

3.1.1. Acceptor reaction products of tetrasaccharide *1*

LC–MS analysis of the α-(1 → 2) transglucosylation products revealed the presence of two GOS, numbered **2** and **3**, corresponding to a pentasaccharide and a hexasaccharide, respectively (Fig. 1). Pentasaccharide **2** was produced during the early stages of the reaction. Its production was correlated with the consumption of tetrasaccharide **1** at an initial velocity of 106 ± 24 μmol min^{-1} mg^{-1} of pure enzyme. For comparison, the initial velocity of concomitant sucrose hydrolysis is 18 μmol min^{-1} mg^{-1}. Hexasaccharide **3**

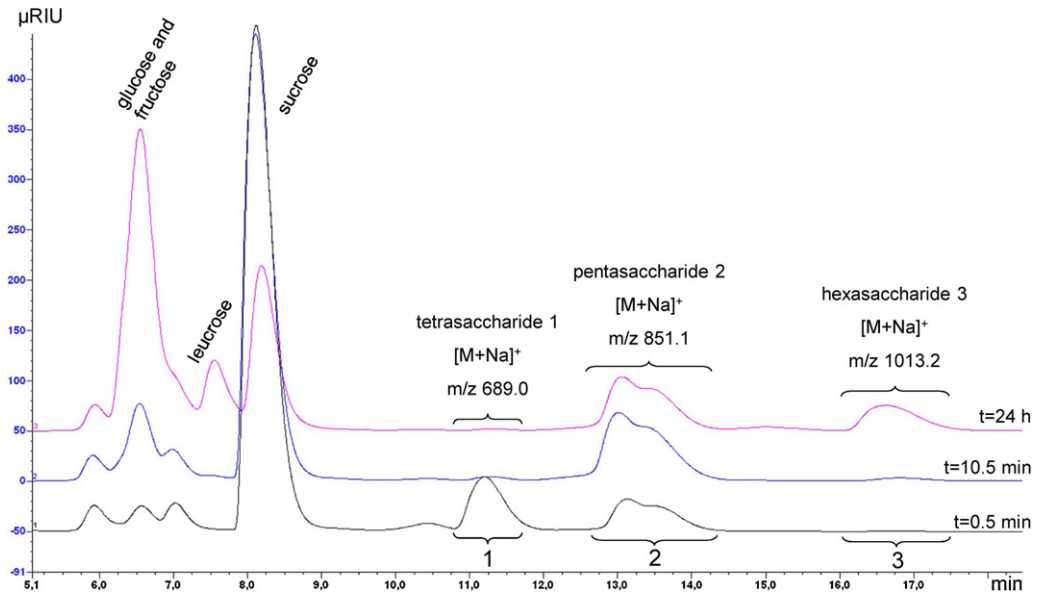

Fig. 1. LC–MS analyses of the α-(1 → 2) GOS obtained with sucrose and tetrasaccharide **1** as acceptor, using GBD-CD2. Numbers refer to the GOS described in this article and to the structures shown in Fig. 2. Time value over each chromatogram indicates the reaction time.

synthesis was delayed, this product being observed only after 53% of tetrasaccharide **1** had been consumed.

Both GOS **2** and **3** were isolated by preparative chromatography and analysed by high resolution mass spectrometry, ^{1}H, HMBC and HMQC NMR spectroscopy (supplementary data, Figs. S2–S6).

These analyses enabled us to unequivocally determine their structures. Pentasaccharide **2,** which corresponds to α-D-Glc*p*-(1 → 2)-α-D-Glc*p*-(1 → 6)-α-D-Glc*p*-(1 → 6)-α-D-Glc*p*-(1 → 4)-D-Glc*p*, was detected as a double peak in Fig. 1. The double peak is due to the separation of the α/β anomers during elution (Dols et al., 1997) This pentasaccharide displays an α-(1 → 2) linked D-Glc*p* unit at its non-reducing end (Fig. 2). More unexpected is the structure of the hexasaccharide **3**, α-D-Glc*p*-(1 → 2)-α-D-Glc*p*-(1 → 6)-[α-D-Glc*p*-(1 → 2)]-α-D-Glc*p*-(1 → 6)-α-D-Glc*p*-(1 → 4)-D-Glc*p*. Indeed, this structure, which has never been described, shows that GBD-CD2 can glucosylate vicinal α-(1 → 6) linked D-Glc*p* units through α-(1 → 2) linkage formation (Fig. 2).

3.1.2. *Acceptor reaction products of pentasaccharide **4***

The LC–MS chromatograms of the reaction medium after 0.5 min incubation revealed the presence of three peaks attributed to the products named **5a**, **5b** and **5c** (Fig. 3).

Their $[M+Na]^+$ adducts correspond to the molecular mass of hexasaccharides (1013.2) (Fig. 3). The initial velocity value of pentasaccharide **4** glucosylation (163 ± 22 µmol min^{-1} mg^{-1}) was higher than that observed for tetrasaccharide **1** (106 ± 24 µmol min^{-1} mg^{-1}). After 7 min reaction, pentasaccharide **4** was totally consumed and additional peaks corresponding to heptasaccharides **6a** and **6b** were observed on the chromatogram. Finally, a peak attributed to octasaccharide **7** was detected after 24 h of reaction (Fig. 3).

The low level of transitory production of the hexasaccharides **5a, 5b** and **5c** has hampered their isolations. To elucidate their structures, the mix of reaction products was submitted to the action of the amyloglucosidase from *A. niger* (supplementary data, Fig. S7). First, we checked that the amyloglucosidase did not hydrolyse the α-(1 → 2) linkage located at the non-reducing extremity of the molecules. As expected, pentasaccharide **4** was totally degraded. In contrast, oligosaccharide **5c** was resistant, indicating that this compound possesses an α-(1 → 2) linkage at its non-reducing end and corresponds to α-D-Glc*p*-(1 → 2)-α-D-Glc*p*-(1 → 6)-α-D-Glc*p*-(1 → 6)-α-D-Glc*p*-(1 → 6)-α-D-Glc*p*-(1 → 4)-D-Glc*p*. Besides, products **5a** and **5b** disappeared during the hydrolysis, with the concomitant formation of two new products identified as double peaks on LC–MS chromatograms, which were attributed to the α/β anomers of tetrasaccharide **0** α-D-Glc*p*-(1 → 2)-α-D-Glc*p*-(1 → 6)-α-D-Glc*p*-(1 → 4)-D-Glc*p* (Remaud-Simeon et al., 1994) and pentasaccharide **2** (supplementary data, Fig. S7). This demonstrates that products **5a** and **5b** are α-D-Glc*p*-(1 → 6)-α-D-Glc*p*-(1 → 6)-[α-D-Glc*p*-(1 → 2)]-α-D-Glc*p*-(1 → 6)-α-D-Glc*p*-(1 → 4)-D-Glc*p* and α-D-Glc*p*-(1 → 6)-[α-D-Glc*p*-(1 → 2)]-α-D-Glc*p*-(1 → 6)-α-D-Glc*p*-(1 → 6)-α-D-Glc*p*-(1 → 4)-D-Glc*p*, respectively (Fig. 4). As shown on the chromatogram obtained after 24 h acceptor reaction, the peaks corresponding to the hexasaccharides (**5a**, **5b** and **5c**) disappeared to give rise to products **6a, 6b** and **7** (Fig. 3). The corresponding $[M+Na]^+$ adducts enable us to propose that products **6a** and **6b** correspond to heptasaccharides. Products **6a** and **6b** were not hydrolysed by amyloglucosidase, indicating that they possess an α-(1 → 2) linkage at their non-reducing ends (supplementary data, Fig. S7). In addition, these products contain a second α-(1 → 2) linked D-Glc*p* unit (supplementary data, Fig. S8). Two possible structures are thus proposed for these products: α-D-Glc*p*-(1 → 2)-α-D-Glc*p*-(1 → 6)-α-D-Glc*p*-(1 → 6)-[α-D-Glc*p*-(1 → 2)]-α-D-Glc*p*-(1 → 6)-α-D-Glc*p*-(1 → 4)-D-Glc*p* or α-D-Glc*p*-(1 → 2)-α-D-Glc*p*-(1 → 6)-[α-D-Glc*p*-(1 → 2)]-α-D-Glc*p*-(1 → 6)-α-D-Glc*p*-(1 → 6)-α-D-Glc*p*-(1 → 4)-D-Glc*p* (Fig. 4).

Octasaccharide **7** (Fig. 3) was isolated. ^{1}H NMR (supplementary data, Fig. S8) and LC–MS unambiguously showed that this compound contains three α-(1 → 2) linked D-Glc*p* units (Fig. 4). Such a structure, α-D-Glc*p*-(1 → 2)-α-D-Glc*p*-(1 → 6)-[α-D-Glc*p*-(1 → 2)]-α-D-Glc*p*-(1 → 6)-[α-D-Glc*p*-(1 → 2)]-α-D-Glc*p*-(1 → 6)-α-D-Glc*p*-(1 → 4)-D-Glc*p*, in which all the α-(1 → 6) linked D-Glc*p* units are α-(1 → 2) branched, has never been described.

Finally, heptasaccharides **6a** and **6b** (10 mM) were tested as acceptors. The initial velocity value of octasaccharide **7** formation was of 8 µmol min^{-1} mg^{-1} showing that the glucosylation of branched products is much less efficient than that of linear ones.

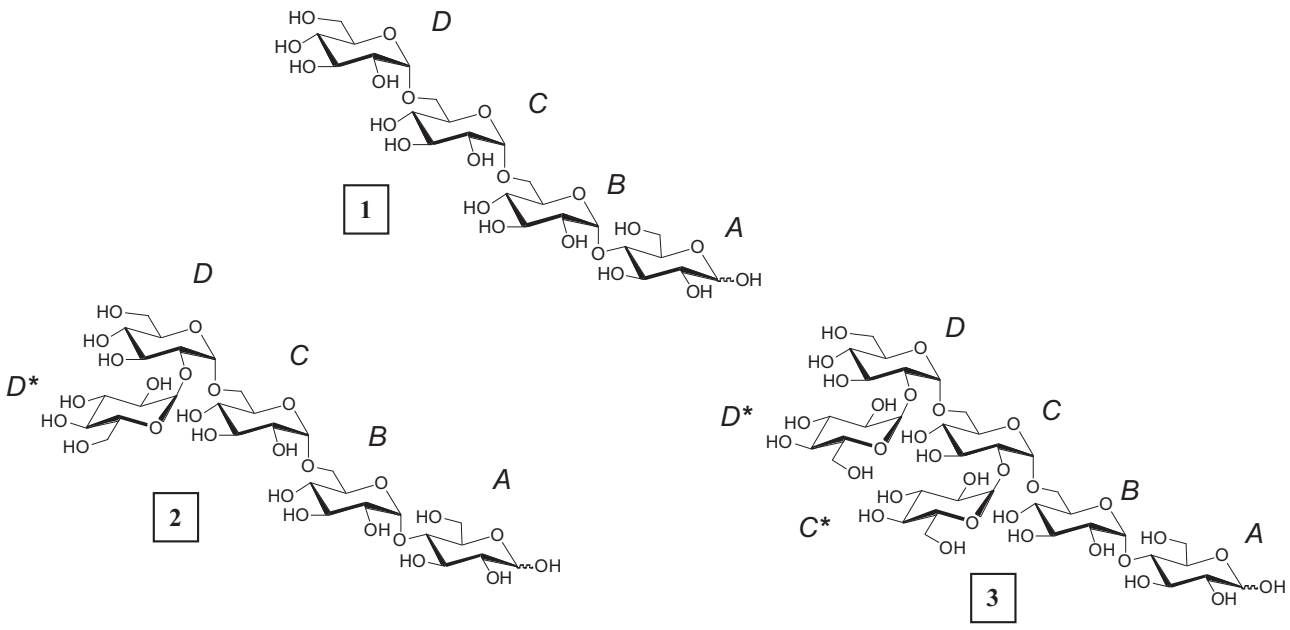

Fig. 2. Structures of the α-(1 → 2) GOS **2** and **3** produced by GBD-CD2 using sucrose and tetrasaccharide **1** as acceptor. Numbers refer to GOS described in the text and to peak attributions in Fig. 3. Uppercase letters refer to D-Glc*p* unit annotations used in NMR spectra (supplementary data, Figs. S2–S6).

Our results demonstrate that branching of acceptors **1** and **4** is sequential and kinetically controlled. In the presence of GOS **1**, the glucosyl units from sucrose are first transferred onto the non-reducing end with the formation of an α-(1 → 2) linkage. The resulting GOS **2** is in turn glucosylated, yielding compound **3**. Unexpectedly, this product possesses two contiguous α-(1 → 2) linkages. The glucosylation of GOS **4** starts with the transitory formation of mono-glucosylated products, which are further glucosylated to produce poly-branched GOS containing several contiguous or non-contiguous α-(1 → 2) branched D-Glc*p* units. The diversity of the acceptor reaction products shows that the first glucosylation event may target any α-(1 → 6) linked D-Glc*p* units.

This observation is in agreement with the ping pong bi bi mechanism previously described for GBD-CD2 and further indicates that pentasaccharide **4** can bind the GBD-CD2 acceptor site in multiple ways (Brison et al., 2010). In addition, the branched products **2**, **5** and **6** can be in turn glucosylated through α-(1 → 2) branching formation showing that both linear and branched GOS substrates can be accommodated in the enzyme active site. The initial velocities of GOS **1** (DP4) and **4** (DP5)

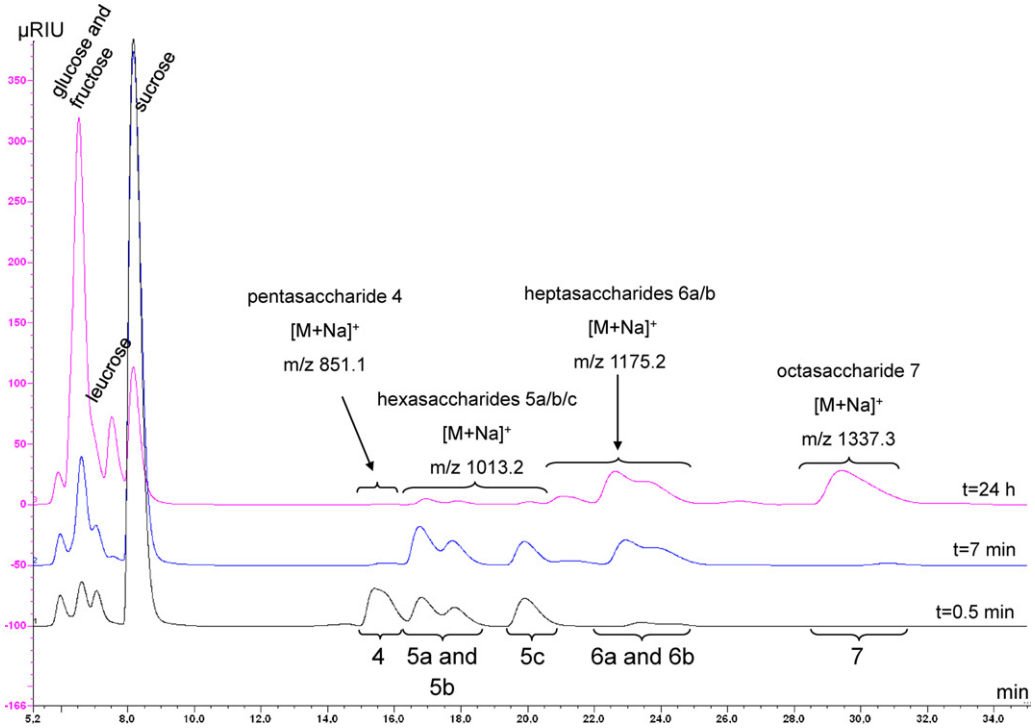

Fig. 3. LC–MS analyses of the α-(1 → 2) GOS obtained with sucrose and pentasaccharide **4** as acceptor using GBD-CD2. Numbers refer to GOS described in this article and to the structures drawn in Fig. 4. Time value printed on each chromatogram indicates the reaction time.

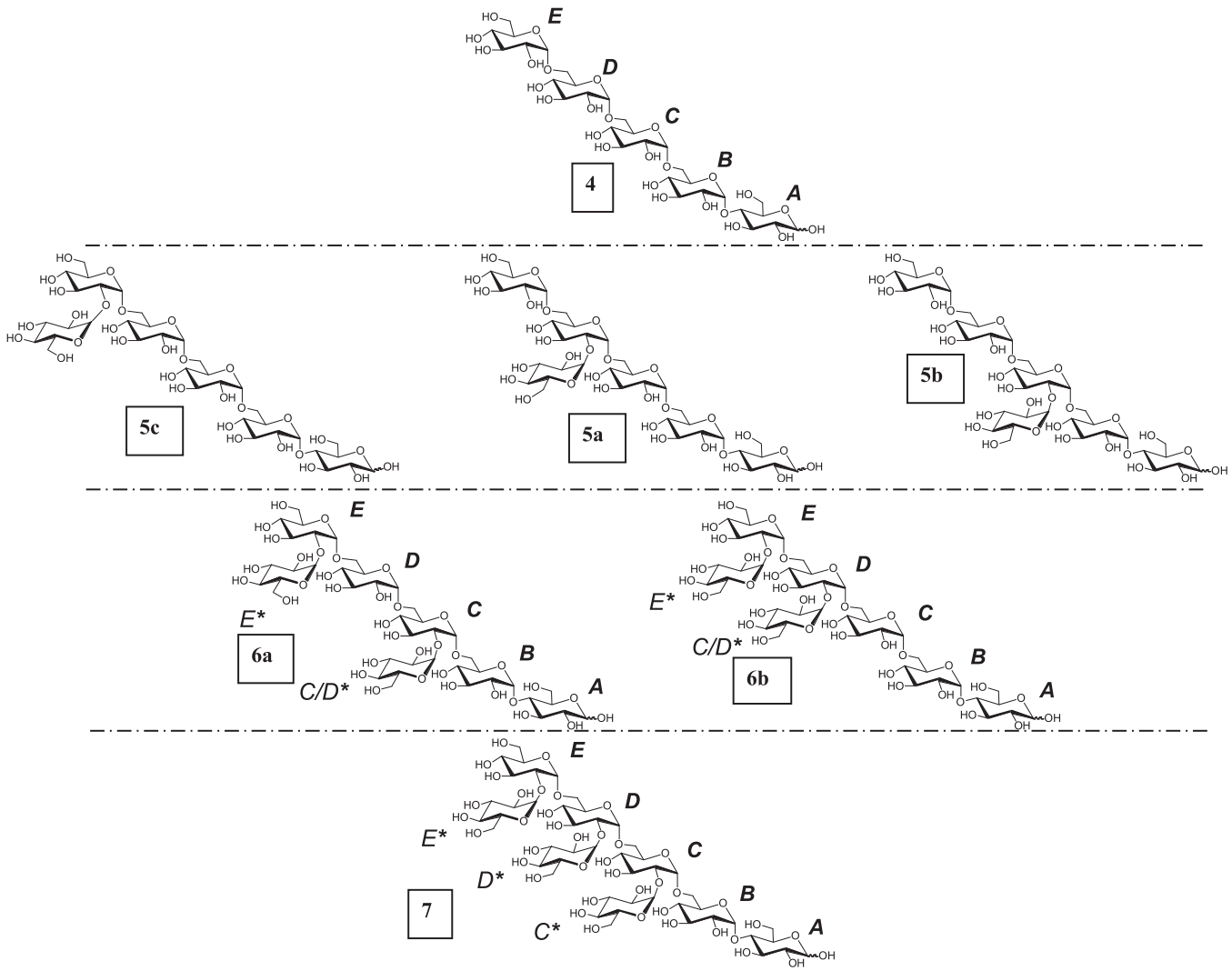

Fig. 4. Structures of the α-(1 → 2) GOS **5a, 5b, 5c, 6a, 6b** and **7** produced by GBD-CD2 using sucrose as donor and pentasaccharide **4** as acceptor. Numbers refer to the GOS described in the text and to peak attributions in Fig. 5. Uppercase letters refer to D-Glc*p* unit annotations in NMR spectra (supplementary data, Fig. S7). Structures **5a**, **5b** and **5c** have been deduced from LC–MS data and chromatogram profiles of the hydrolysis reaction using *Aspergillus niger* amyloglucosidase (supplementary data, Fig. S6).

consumptions are respectively of $106 \pm 24\ \mu mol\ min^{-1}\ mg^{-1}$ and $163 \pm 22\ \mu mol\ min^{-1}\ mg^{-1}$, suggesting that the transfer onto the longest α-(1 → 6)-linked acceptors is kinetically favoured. Glucosylation of the branched acceptors is possible but not kinetically favoured (octasaccharide **7** formation rate = $8\ \mu mol\ min^{-1}\ mg^{-1}$). This result can probably be attributed to difficulties of binding at the acceptor site.

3.2. α-(1 → 2) branching of 1.5 kDa dextran

The 1.5 kDa dextran that was used as acceptor is composed of a population of IMOS of DP ranging from 1 to 61 (Fig. 5). To modulate the α-(1 → 2) linkage content of the glucosylation products, various [sucrose]/[dextran] molar ratios were used, as previously described (Brison et al., 2010). The branched dextrans containing between 0% and 25% of α-(1 → 2) linkages were then submitted to the action of the exo-acting amyloglucosidase from *A. niger* and the endo-acting endodextranase from *C. gracile*. Both enzymes do not hydrolyse α-(1 → 2) bonds. As shown in Fig. 5, HPAEC-PAD chromatograms of the α-(1 → 2) branched dextrans before and after glucoamylase hydrolysis show that the resistance to glucoamylase hydrolysis increases with the increase of the α-(1 → 2) bond ratio.

Indeed, the hydrolysis ratio decreases almost linearly from 97% to 21% when the α-(1 → 2) linkage contents increases from 0 to 25.5% (supplementary data, Fig. S9). In addition, as shown in Fig. 6, the presence of the α-(1 → 2) linkages confers a high resistance to the endodextranase action. The 1.5 kDa dextran with 26% of branching is almost totally resistant to this enzyme.

3.2.1. Simulation of the branching reaction

To graft a polydisperse population of dextran, the enzyme GBD-CD2 may adopt several modes of action. The enzyme may preferentially select the shorter chains (or the longer ones), and the branching event may be an ordered or a random process. A specific pattern of branching could also be envisaged that could be inferred by the topology of the active site and the way the dextran binds to the acceptor sites. To get insight in this process, we have simulated various branching scenarios according to three criteria (i) the chain selection by the enzyme, (ii) the direction of branching progression and (iii) the branching pattern. Then, programme implementation also enabled the degradation of the branched dextran by glucoamylase to be simulated and the results to be compared to experimental data. The results of these models are reported in Table 2. Modelling results have been split in

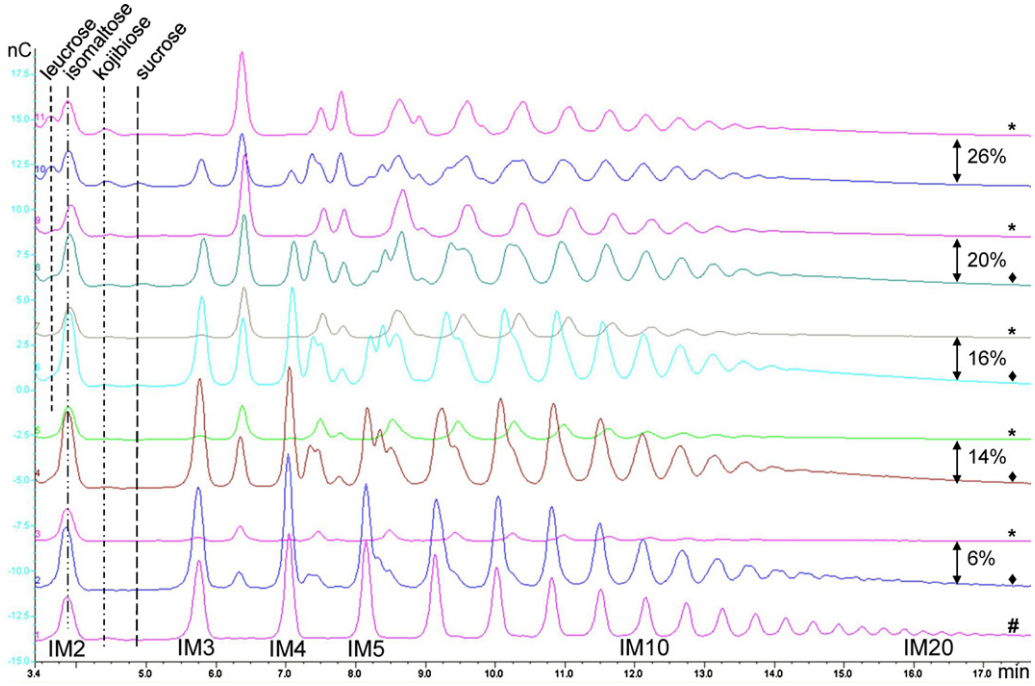

Fig. 5. Superimposition of HPAEC-PAD chromatograms of dextrans, with controlled amounts of α-(1 → 2) branches (synthesized in the presence of dextran 1.5 kDa and sucrose) and of their hydrolysis products obtained with *Aspergillus niger* amyloglucosidase. (#) dextran 1.5 kDa standard; (♦), (*) α-(1 → 2) branched dextrans before and after amyloglucosidase hydrolysis, respectively. Percentages indicated on the right part of this figure correspond to the ratios of α-(1 → 2) linked glucosyl units to the total amount of glucosyl units in branched dextrans. IM2–IM20 correspond to the isomalto-oligosaccharides of degree of polymerization from 2 to 20.

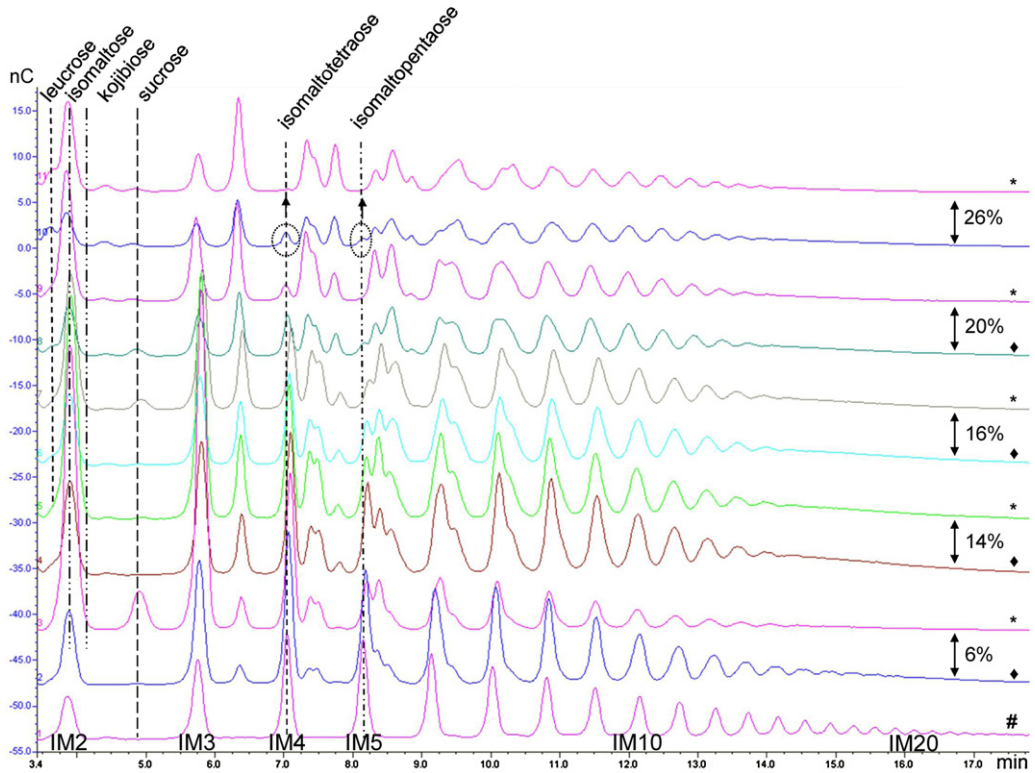

Fig. 6. Superimposition of HPAEC-PAD chromatograms of dextrans, with controlled amounts of α-(1 → 2) branches (synthesized from dextran 1.5 kDa and sucrose) and of their hydrolysis products obtained with *Chaetomium gracile* endodextranase. (#) dextran 1.5 kDa standard; (♦), (*) α-(1 → 2) branched dextrans before and after the endodextranase hydrolysis, respectively. Percentages indicated on the right part of this figure correspond to the ratios of α-(1 → 2) linked glucosyl units to the total amount of glucosyl units in branched dextrans. IM2–IM20 correspond to the isomalto-oligosaccharides of degree of polymerization from 2 to 20.

Table 2
Modelling of α-(1 → 2) branching of 1.5 kDa dextran by GBD-CD2. *In silico* results are classified in three groups depending on the sum of squared differences between experimental and *modelled* results. Grey, sums higher than 2.5%; light grey, sums ranging from 0.6 to 2.0%; white, sums lower than 0.5%. Exp. stands for the experimental results of amyloglucosidase digestion of α-(1 → 2) branched dextrans. Ø stands for calculations that could not converge.

α-(1→2) linkage in dextran (%)	Exp.	Scenarios																			
		A	G	N	O	B	C	D	H	I	J	M	Q	P	E	F	K	L	R	S	T
	% of glucose released by amyloglucosidase hydrolysis of α 1→2) branched dextrans																				
0	95	100	100	100	100	100	100	100	100	100	100	100	100	100	100	100	100	100	100	100	100
6.2	84	79	79	76	74	71	78	75	71	78	75	77	71	72	69	90	69	90	90	90	90
13.7	62	54	54	56	51	42	50	45	42	50	45	58	51	45	39	76	39	76	76	76	76
16.3	42	42	42	46	40	30	36	30	30	36	30	49	42	33	26	68	26	68	68	68	68
19.9	32	32	32	38	30	21	24	19	21	24	19	41	34	22	17	60	17	60	60	60	60
25.6	21	21	21	28	18	13	14	Ø	13	14	Ø	31	26	Ø	9	50	9	50	50	50	50
	(Sum of squares of differences between experimental percentage of released glucose, in branched dextrans, and simulations)/5 × 100																				
		0.2	0.2	0.5	0.5	1.7	0.6	2.1	1.7	0.6	2.1	0.7	0.7	2.0	2.6	5.4	2.6	5.4	5.4	5.4	5.4

three groups based on the sum of squared differences between the experimental percentage of released glucose and the model data. Scenarios E, F, K, L, R, S and T are the most divergent from the experimental data. They all include a specific branching direction from the reducing or the non-reducing end of oligodextran chains. The intermediate group consists of scenarios B, C, D, H, I, J, M, Q and P. This group, excepted for scenarios M and Q, contains scenarios that all consider a specific branching pattern along the linear dextran chains.

The third group of simulations, for which simulated and experimental results are the closest, encompasses scenarios A, G, N and O, all characterized by (i) a random selection of the chains to be branched, (ii) a random branching direction and (iii) no particular branching pattern excepted for scenario O for which one gap between each α-(1 → 2) branch is present.

These results indicate that the enzyme would not show a marked preference for a specific degree of polymerization and that the branching reaction is a stochastic process. They further confirm that each IMOS of defined DP can bind the active site in various ways. These results based on 1.5 kDa dextran branching are also consistent with the kinetic data and structures obtained from GOS **4,** which show that there is no specific position for the first α-(1 → 2) branching event.

4. Conclusion

Branching of individual GOS of defined DP revealed that GBD-CD2 can accommodate both linear and α-(1 → 2) branched products as acceptors, the glucosylation of linear GOS being kinetically preferred. Structural characterization of the reaction products revealed that α-(1 → 2) branching may also occur on adjacent α-(1 → 6) linked glucosyl units after successive glucosylation reactions, resulting in new comb-like structures. In addition, the results of our simulations all converge to the conclusion that GDB-CD2 performs branching at random positions along IMOS chains. This is consistent with the GDB-CD2 ping pong bi bi mechanism and is also supported by the kinetic analysis of pentasaccharide **4** glucosylation which revealed the transitory formation of GOS that are branched on various α-(1 → 6) linked D-Glc*p* units. This reveals that GBD-CD2 active site is flexible towards acceptor structures, at least for IMOS of DP varying from 2 to 31, and that the α-(1 → 2) D-Glc*p* units may be randomly positioned along the chains. These investigations combined to the X-ray structural analysis of the enzyme in complex with linear or branched GOS that would be obtained, will now be used to improve enzyme selectivity through enzyme engineering and to drive processes of α-(1 → 2) branched GOS production in order to generate novel functional foods.

Acknowledgements

This work was financially supported by a grant from the region Midi-Pyrénées, France. We thank Pierre Escalier for technical assistance.

Appendix A. Supplementary data

Supplementary data associated with this article can be found, in the online version, at doi:10.1016/j.carbpol.2013.01.064.

References

André, I., Potocki-Véronèse, G., Morel, S., Monsan, P., & Remaud-Siméon, M. (2010). *Sucrose-utilizing transglucosidases for biocatalysis. Carbohydrates in Sustainable Development I* Berlin/Heidelberg: Springer., pp. 1–25

Bertrand, A., Morel, S., Lefoulon, F., Rolland, Y., Monsan, P., & Remaud-Simeon, M. (2006). *Leuconostoc mesenteroides* glucansucrase synthesis of flavonoid glucosides by acceptor reactions in aqueous-organic solvents. *Carbohydrate Research*, *341*(7), 855–863.

Boucher, J., Daviaud, D., Simeon-Remaud, M., Carpene, C., Saulnier-Blache, J. S., Monsan, P., et al. (2003). Effect of non-digestible gluco-oligosaccharides on glucose sensitivity in high fat diet fed mice. *Journal of Physiology and Biochemistry*, *59*(3), 169–173.

Bounaix, M. S., Gabriel, V., Morel, S., Robert, H., Rabier, P., Remaud-Siméon, M., et al. (2009). Biodiversity of exopolysaccharides produced from sucrose by sourdough lactic acid bacteria. *Jounal of Agricultural and Food Chemistry*, *57*, 10889–10897.

Bozonnet, S., Dols-Laffargue, M., Fabre, E., Pizzut, S., Remaud-Simeon, M., Monsan, P., et al. (2002). Molecular characterization of DSR-E, an alpha-1,2 linkage-synthesizing dextransucrase with two catalytic domains. *Journal of Bacteriology*, *184*(20), 5753–5761.

Brison, Y., Fabre, E., Moulis, C., Portais, J.-C., Monsan, P., & Remaud-Siméon, M. (2010). Synthesis of dextrans with controlled amounts of α-1,2 linkages using the transglucosidase GBD–CD2. *Applied Microbiology and Biotechnology*, *86*(2), 545–554.

Brison, Y., Pijning, T., Malbert, Y., Fabre, E., Mourey, L., Morel, S., et al. (2012). Functional and structural characterization of an α-(1 → 2) branching sucrase derived from DSR-E glucansucrase. *Journal of Biological Chemistry*, *287*(11), 7915–7924.

Cantarel, B. L., Coutinho, P. M., Rancurel, C., Bernard, T., Lombard, V., & Henrissat, B. (2009). The carbohydrate-active enzymes database (CAZy): an expert resource for glycogenomics. *Nucleic Acids Research*, *37*(Suppl. 1), D233–D238.

Côté, G. L., Dunlap, C. A., & Vermillion, K. E. (2009). Glucosylation of raffinose via alternansucrase acceptor reactions. *Carbohydrate Research*, *344*(15), 1951–1959.

Djouzi, Z., & Andlueux, C. (1997). Compared effects of three oligosaccharides on metabolism of intestinal microflora in rats inoculated with a human faecal flora. *British Journal of Nutrition*, *78*(2), 313–324.

Dols, M., Simeon, M. R., Willemot, R. M., Vignon, M. R., & Monsan, P. F. (1997). Structural characterization of the maltose acceptor-products synthesized by *Leuconostoc mesenteroides* NRRL B-1299 dextransucrase. *Carbohydrate Research*, *305*(3–4), 549–559.

Fabre, E., Bozonnet, S., Arcache, A., Willemot, R. M., Vignon, M., Monsan, P., et al. (2005). Role of the two catalytic domains of DSR-E dextransucrase and their involvement in the formation of highly alpha-1,2 branched dextran. *Journal of Bacteriology*, *187*(1), 296–303.

Flickinger, E. A., Wolf, B. W., Garleb, K. A., Chow, J., Leyer, G. J., Johns, P. W., et al. (2000). Glucose-based oligosaccharides exhibit different in vitro fermentation patterns and affect in vivo apparent nutrient digestibility and microbial populations in dogs. *Journal of Nutrition*, *130*(5), 1267–1273.

Hattori, A., Ishibashi, K., & Minato, S. (1981). The purification and characterization of the dextranase of *Chaetomium gracile*. *Agricultural and Biological Chemistry*, *45*(11), 2409–2416.

Henrissat, B., & Davies, G. (1997). Structural and sequence-based classification of glycoside hydrolases. *Current Opinion in Structural Biology*, *7*(5), 637–644.

Iliev, I., Vassileva, T., Ignatova, C., Ivanova, I., Haertlé, T., Monsan, P., et al. (2008). Gluco-oligosaccharides synthesized by glucosyltransferases from constitutive mutants of *Leuconostoc mesenteroides* strain Lm 28. *Journal of Applied Microbiology*, *104*(1), 243–250.

Kobayashi, I., & Matsuda, K. (1977). Structural characteristics of dextran synthesized by *Leuconostoc mesenteroides* NRRL B-1299. *Agricultural and Biological Chemistry*, *41*, 1931–1937.

Lopez, A., & Monsan, P. (1980). Dextran synthesis by immobilized dextran sucrase. *Biochimie*, *62*(5–6), 323–329.

Malik, A., Radji, M., Kralj, S., & Dijkhuizen, L. (2009). Screening of lactic acid bacteria from Indonesia reveals glucansucrase and fructansucrase genes in two different *Weissella confusa* strains from soya. *FEMS Microbiology Letters*, *300*(1), 131–138.

Monchois, V., Willemot, R. M., & Monsan, P. (1999). Glucansucrases: mechanism of action and structure-function relationships. *FEMS Microbiology Reviews*, *23*(2), 131–151.

Moon, Y. H., Nam, S. H., Kang, J., Kim, Y. M., Lee, J. H., Kang, H. K., et al. (2007). Enzymatic synthesis and characterization of arbutin glucosides using glucansucrase from *Leuconostoc mesenteroides* B-1299CB. *Applied Microbiology and Biotechnology*, *77*(3), 559–567.

Mooser, G., Hefta, S. A., Paxton, R. J., Shively, J. E., & Lee, T. D. (1991). Isolation and sequence of an active-site peptide containing a catalytic aspartic acid from two *Streptococcus sobrinus* alpha-glucosyltransferases. *Journal of Biological Chemistry*, *266*(14), 8916–8922.

Paul, F., Oriol, E., Auriol, D., & Monsan, P. (1986). Acceptor reaction of a highly purified dextransucrase with maltose and oligosaccharides. Application to the synthesis of controlled-molecular-weight dextrans. *Carbohydrate Research*, *149*(2), 433–441.

Pazur, J. H., & Ando, T. (1960). The hydrolysis of glucosyl oligosaccharides with alpha-(1 → 4) and alpha-(1 → 6) bonds by fungal amyloglucosidase. *Journal of Biological Chemistry*, *235*(2), 297–302.

Remaud-Simeon, M., Lopez-Munguia, A., Pelenc, V., Paul, F., & Monsan, P. (1994). Production and use of glucosyltransferases from *Leuconostoc mesenteroides* NRRL B-1299 for the synthesis of oligosaccharides containing α-(1 → 2) linkages. *Applied Biochemistry and Biotechnology*, *44*(2), 101–117.

Sanz, M. L., Côté, G. L., Gibson, G. R., & Rastall, R. A. (2006). Influence of glycosidic linkages and molecular weight on the fermentation of maltose-based oligosaccharides by human gut bacteria. *Journal of Agricultural and Food Chemistry*, *54*(26), 9779–9784.

Sarbini, S. R., Kolida, S., Naeye, T., Einerhand, A., Brison, Y., Remaud-Simeon, M., et al. (2011). In vitro fermentation of linear and α-1, 2-branched dextrans by the human fecal microbiota. *Applied and Environmental Microbiology*, *77*(15), 5307–5315.

Serino, M., Luche, E., Gres, S., Baylac, A., Bergé, M., Cenac, C., et al. (2012). Metabolic adaptation to a high-fat diet is associated with a change in the gut microbiota. *Gut*, *61*(4), 543–553.

Seymour, F. R., Knapp, R. D., Chen, E. C. M., Bishop, S. H., & Jeanes, A. (1979). Structural analysis of *Leuconostoc* dextrans containing 3-*O*-α-glucosylated α-glucosyl residues in both linear-chain and branch-point positions, or only in branch-point positions, by methylation and by ^{13}C NMR spectroscopy. *Carbohydrate Research*, *74*(1), 41–62.

Sumner, J., & Howells, S. (1935). A method for determination of invertase activity. *Journal of Biological Chemistry*, *108*, 51–54.

Valette, P., Pelenc, V., Djouzi, Z., Andrieux, C., Paul, F., Monsan, P., et al. (2006). Bioavailability of new synthesised glucooligosaccharides in the intestinal tract of gnotobiotic rats. *Journal of the Science of Food and Agriculture*, *62*, 121–127.

van Hijum, S. A., Kralj, S., Ozimek, L. K., Dijkhuizen, L., & van Geel-Schutten, I. G. (2006). Structure-function relationships of glucansucrase and fructansucrase enzymes from lactic acid bacteria. *Microbiology and Molecular Biology Reviews*, *70*(1), 157–176.

Vujičić-Žagar, A., Pijning, T., Kralj, S., Lopez, C. A., Eeuwema, W., Dijkhuizen, L., et al. (2010). Crystal structure of a 117 kDa glucansucrase fragment provides insight into evolution and product specificity of GH70 enzymes. *Procedings of the National Academy of Sciences of the United States of America*, *107*(50), 21406–21411.